

Complex evolution of the electronic structure of Cr with temperature

Ganesh Adhikary, R. Bindu, Swapnil Patil, and Kalobaran Maiti

Citation: *Appl. Phys. Lett.* **100**, 042401 (2012); doi: 10.1063/1.3678183

View online: <http://dx.doi.org/10.1063/1.3678183>

View Table of Contents: <http://apl.aip.org/resource/1/APPLAB/v100/i4>

Published by the [American Institute of Physics](#).

Related Articles

A suspended nanogap formed by field-induced atomically sharp tips
Appl. Phys. Lett. **101**, 183106 (2012)

Corrugated flat band as an origin of large thermopower in hole doped PtSb₂
AIP Advances **2**, 042108 (2012)

Beam waves in tungsten
Low Temp. Phys. **38**, 442 (2012)

Investigation of the structural, electronic, and magnetic properties of Ni-based Heusler alloys from first principles
J. Appl. Phys. **111**, 033905 (2012)

Electronic structure and symmetry of valence states of epitaxial NiTiSn and NiZr_{0.5}Hf_{0.5}Sn thin films by hard x-ray photoelectron spectroscopy
Appl. Phys. Lett. **99**, 221908 (2011)

Additional information on *Appl. Phys. Lett.*

Journal Homepage: <http://apl.aip.org/>

Journal Information: http://apl.aip.org/about/about_the_journal

Top downloads: http://apl.aip.org/features/most_downloaded

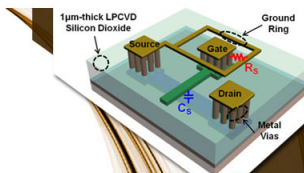
Information for Authors: <http://apl.aip.org/authors>

ADVERTISEMENT



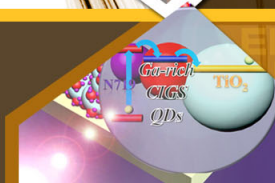
**EXPLORE WHAT'S
NEW IN APL**

SUBMIT YOUR PAPER NOW!



SURFACES AND INTERFACES

Focusing on physical, chemical, biological, structural, optical, magnetic and electrical properties of surfaces and interfaces, and more...



ENERGY CONVERSION AND STORAGE

Focusing on all aspects of static and dynamic energy conversion, energy storage, photovoltaics, solar fuels, batteries, capacitors, thermoelectrics, and more...

Complex evolution of the electronic structure of Cr with temperature

Ganesh Adhikary, R. Bindu, Swapnil Patil, and Kalobaran Maiti^{a)}

Department of Condensed Matter Physics and Materials Science, Tata Institute of Fundamental Research, Homi Bhabha Road, Colaba, Mumbai - 400 005, India

(Received 1 November 2011; accepted 23 December 2011; published online 23 January 2012)

Employing state-of-the-art high resolution photoemission spectroscopy, we studied the electronic structure evolution of Cr with temperature. Experimental results reveal signature of a pseudogap much below the spin density wave transition temperature. A sharp peak appears near the Fermi level at low temperatures presumably related to the orbital Kondo effect. These results provide possible origin of the complex electronic properties observed in this system. © 2012 American Institute of Physics. [doi:10.1063/1.3678183]

Among elemental metals, chromium is one of the most important element, which is used in varieties of applications such as metallurgical applications, making dye and pigments, catalysis, tanning, refractory materials, magnetic tapes and recording media, thermocouple etc., due to its interesting but complex electronic properties. For example, Cr is an archetypical example of Fermi surface nesting driven antiferromagnet¹ exhibiting incommensurate spin density wave (SDW) transition at 311 K, which can be suppressed to 0 K by small ($\sim 3.5\%$) V doping.² Various studies derived the Fermi surface nesting vector in the SDW phase for both bulk and surface electronic structures.^{3–6} An infrared reflectivity study predicted multiple gaps (a direct gap of 125 meV and an indirect gap of 450 meV (Ref. 7)) or pseudo-gap in SDW phase as predicted theoretically.⁸ A scanning tunneling microscopic measurements showed orbital Kondo resonance in Cr.⁹ Subsequent studies^{10,11} indicated varied scenarios involving Kondo interactions, electron-phonon coupling, Shockley-type surface state formation, etc. Evidently, an elemental metal, Cr possess complexity associated to widely discussed quantum phase transitions in unconventional superconductors, heavy fermions etc.

Here, we studied temperature evolution of the electronic structure of Cr employing *state of the art* high resolution photoemission spectroscopy. Measurements were carried out on high purity *in situ* scraped sample using monochromatic He I (21.2 eV), He II (40.8 eV), and Al K α (1486.6 eV) photon sources and SES2002 Gammadata Scienta analyzer with the energy resolution set to 2.5 meV, 5 meV, and 350 meV, respectively, at a base pressure $< 3 \times 10^{-11}$ Torr. The energy dispersive analysis of x-rays using a scanning electron microscope (SEM) and photoemission measurements do not exhibit detectable impurity suggesting the level of impurity, if any, is below 1%. SEM images of as prepared surface shown in Figs. 1(a) and 1(b) exhibit a smooth surface. The SEM image of the sputtered—annealed surface is shown in Fig. 1(c) exhibiting improved surface quality. However, the bulk photoemission spectra were found not to be influenced by the surface preparation as expected for such measurements with a spot size of about 1 mm.

In Fig. 1(d), we show the energy band structure of Cr calculated using full potential linearized augmented plane wave method within the local spin density approximations.¹² 4s and 4p contributions appear at higher binding energies (> 3 eV) and the Fermi surface is formed by 3d electronic states. Around Γ point, the energy bands forming electron pockets has t_{2g} symmetry and hole pockets possess e_g symmetry. The SDW gap, observed earlier,⁴ forms via folding of the t_{2g} bands while the e_g bands cross the Fermi level, ϵ_F retaining the metallicity at low temperatures. We have convoluted the sum of the photoemission cross section weighted partial density of states with the Fermi-Dirac distribution function to extract the occupied part and a gaussian representing the energy resolution for Al K α measurements. Resulting spectrum shown in Fig. 1(e) captures almost all the features of the Al K α valence band spectrum—a weak intensity around 6 eV shown by the arrow in the figure may appear due to asymmetric lineshape arising from energy dependent life time broadening, low energy excitations in the photoemission final states, or a signature of electron correlation induced lower Hubbard band¹³ as found in other transition metals such as Ni.¹⁴ Correlation effect cannot be ignored as it possess finite magnetic moment—a result of effective local character of 3d electrons. The signature of electron correlation also appears as satellites in the core level spectra.¹⁵ The Cr 2p spectrum shown in Fig. 1(f) exhibits two features corresponding to the spin-orbit split $2p_{3/2}$ and $2p_{1/2}$ signals with intensity ratio commensurate to their multiplicity of 2:1. No intensity for the correlation induced satellite is observed suggesting that the electron correlation, if present in this system, is significantly weak.¹⁶

Since the valence electronic states possess essentially Cr 3d character, the photoemission cross-section will be a multiplicative factor to intensity. Therefore, a comparison of the valence band spectra collected with different photon energies (see Fig. 2(a)) manifests the surface-bulk differences in the electronic structure.¹⁷ To consider the differences in resolution broadening in various experimental techniques, we superimposed the resolution broadened He I spectrum (line) over the Al K α spectrum (open circles). The He I spectrum exhibits higher intensities of the features S1 and S2, while features B1 and B2 are dominant in the Al K α spectrum. The electron mean free path at ultraviolet energies is lower than that in x-ray energies.¹⁷ Thus, S1 and S2 can be identified as

^{a)} Author to whom correspondence should be addressed. Electronic mail: kbmaiti@tifr.res.in.

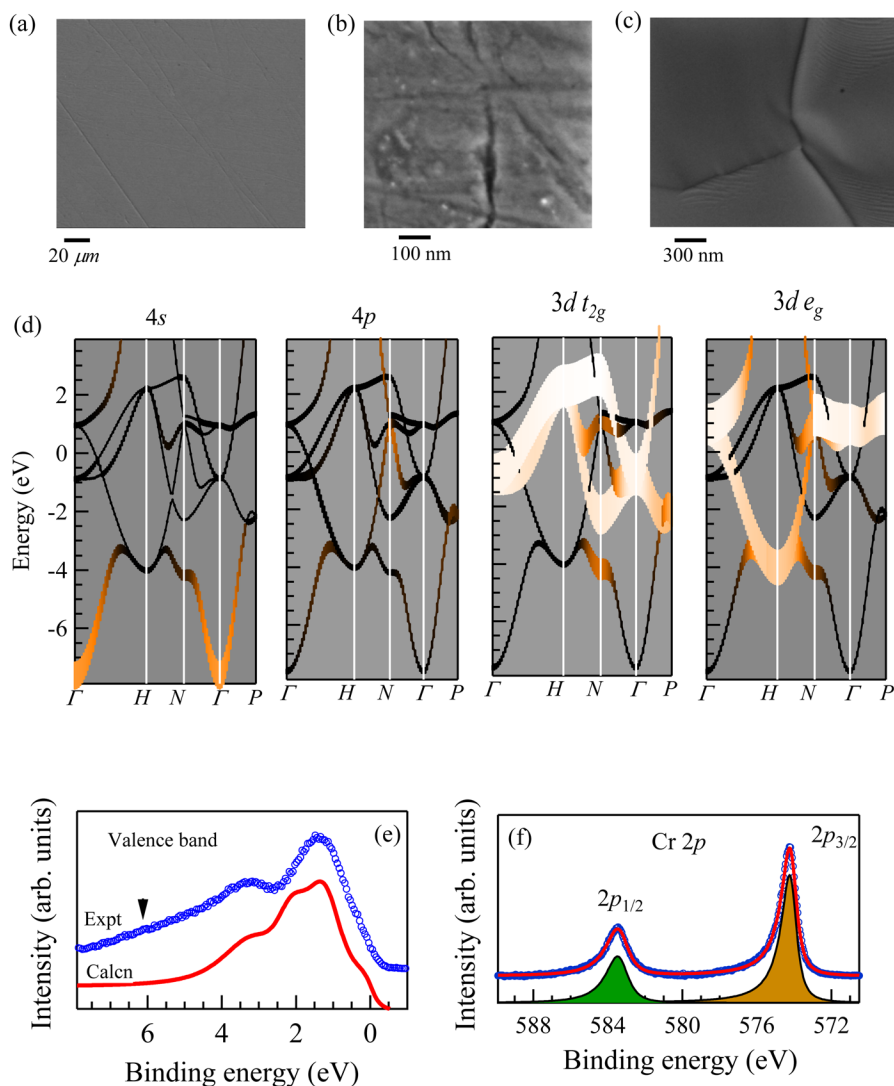


FIG. 1. (Color online) SEM picture of polished surface in (a) μm and (b) nm scale close to grain boundary. (c) SEM image after sputter-anneal cycle. (d) Calculated band dispersions—the thickness of the line represents the orbital contributions. (e) Spectral function calculated from band structure results (line) is compared with the Al $K\alpha$ spectrum (symbols). (f) Cr $2p$ spectrum (symbols), the fit (line over the symbols), and the components, $2p_{3/2}$ and $2p_{1/2}$ peaks (area plots).

the surface features and possess d_{z^2} and $d_{x^2-y^2}$ character, respectively, consistent with the earlier observations.^{5,6} The features B1 and B2 correspond to the bulk electronic structure.

Considering complex phase transitions observed in Cr as a function of temperature, it is important to investigate how the above features evolves with temperature. In Fig. 2(b), the Al $K\alpha$ spectra at different temperatures are very similar indicating the temperature insensitivity of the bulk electronic structure in the high energy scale. On the other hand, the He II and He I spectra (see Figs. 2(c) and 2(d)) show that the intensity of S1 relative to S2 reduces gradually with the decrease in temperature. The bulk features remain almost the same, consistent with the observation in the Al $K\alpha$ spectra. Note that at these high binding energies, the large life time broadening (≥ 0.5 eV) makes the difference in resolution broadening in various techniques irrelevant. Earlier study⁶ suggested that the surface states exhibit ferromagnetism with a Curie temperature as high as 780 K. The exchange interaction strength among the surface states increases gradually with the decrease in temperature. Therefore, the eigen energies of the minority and majority spin states gradually move away from ϵ_F leading to an effective depletion of S1.⁶ Consequently, the contribution of the sur-

face states at ϵ_F gradually becomes insignificant at low temperatures. Since the t_{2g} states already form a gap below SDW transition temperature, the major contribution at ϵ_F at low temperatures will be due to the Cr $3d$ bulk states possessing e_g symmetry.

Since, the resolution broadening (FWHM = 2.5 meV) is small compared to the energy scale of investigation, $I(\epsilon)/F(\epsilon, T)[I(\epsilon) = \text{photoemission intensity}, F(\epsilon, T) = \text{resolution broadened Fermi Dirac function, (FDDF)}]$ is a good representation of the spectral density of states (SDOS). The spectral intensity at ϵ_F can also be estimated by symmetrization of the experimental spectra $[I(\epsilon) = I(\epsilon - \epsilon_F) + I(\epsilon_F - \epsilon)]$. The temperature evolution of the Ag spectra shown in Fig. 3(a) manifests the high resolution of the technique; ϵ_F is derived from these spectra. We observe that SDOS of Ag obtained via symmetrization of the spectra in Fig. 3(b) and division by FDDF in Fig. 3(c) are almost identical indicating robustness of the procedures—a small dip at ϵ_F at 15 K often found in condensed matter systems due to disorder.^{18,19}

The temperature evolution of the valence band spectra and SDOS obtained by FDDF division for Cr are shown in Figs. 3(d) and 3(e). SDOS at 325 K and 295 K exhibit signature of a peak around 75 meV above ϵ_F —presumably $3d_{z^2}$ peak as predicted earlier.⁶ The intensity at ϵ_F initially

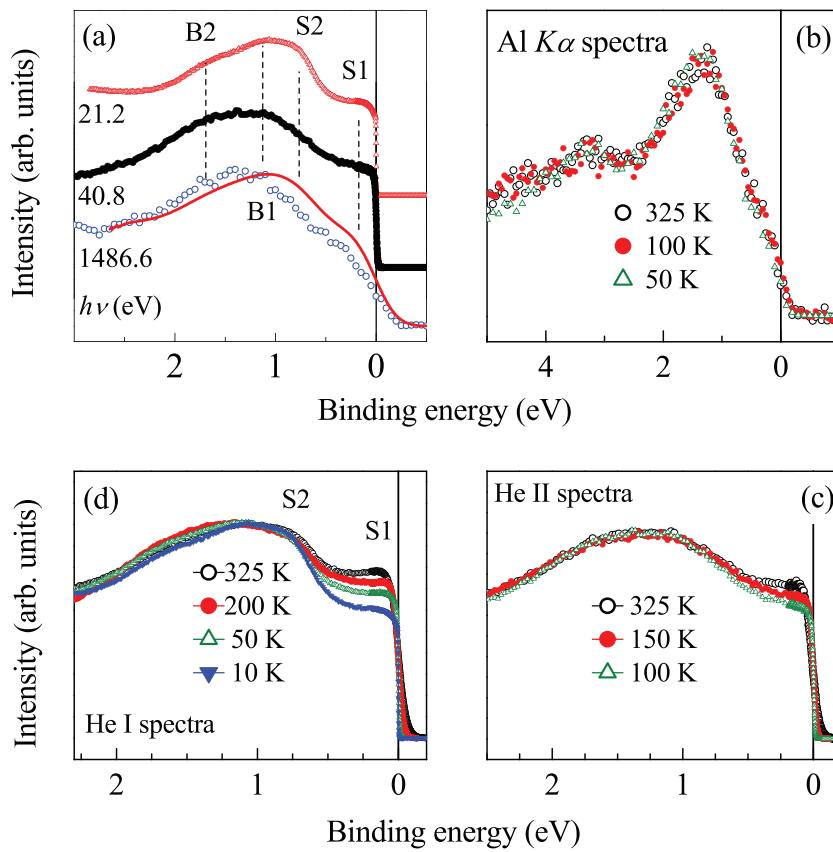


FIG. 2. (Color online) (a) Valence band spectra at different photon energies. Line is the broadened He I spectrum. Temperature dependence of the valence band spectra at (b) Al $K\alpha$, (c) He II, and (d) He I photon energies.

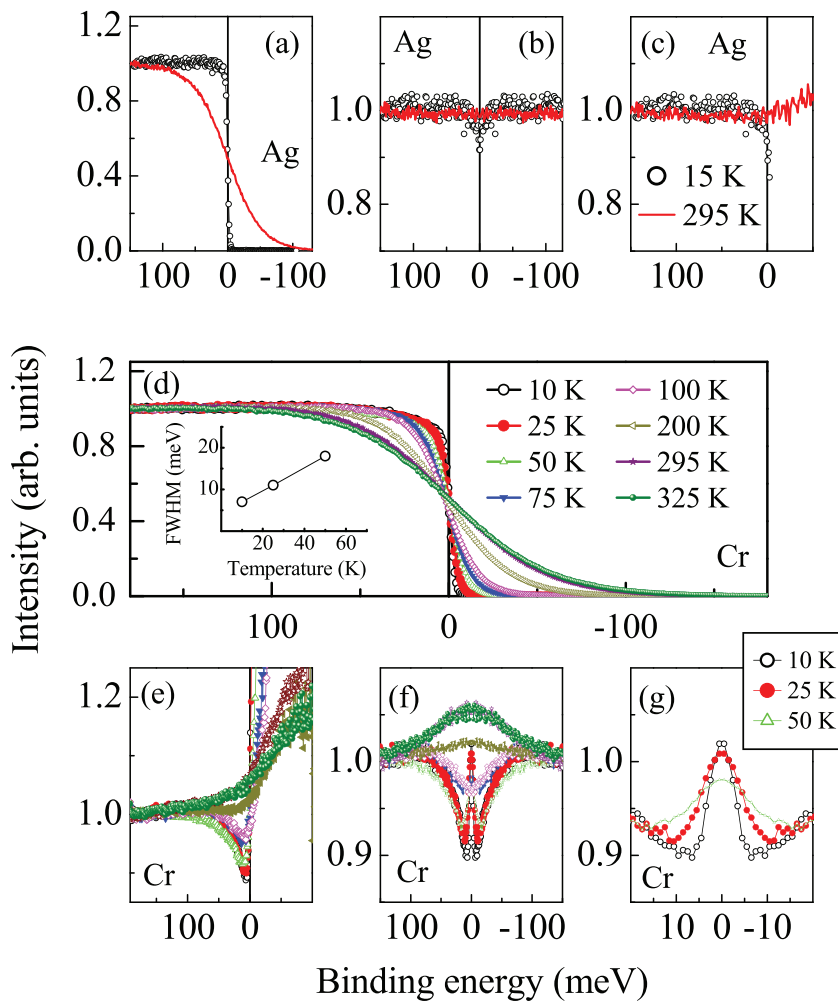


FIG. 3. (Color online) (a) Valence band spectra of Ag at 15 K (symbols) and 295 K (line). Ag SDOS obtained via (b) symmetrization and (c) FDDF division of the raw spectra. (d) Valence band spectra of Cr. Cr SDOS obtained via (e) FDDF division and (f) symmetrization. (g) The symmetrized SDOS at $T \leq 50$ K. The peak width is shown as a function of temperature in the inset of (d).

reduces gradually with the decrease in temperature and then increases below 50 K revealing a peak above ϵ_F . The SDOS obtained by symmetrization of the raw data shown in Fig. 3(f) exhibit a broad peak at 325 K (paramagnetic phase). At 295 K (below the SDW transition), the spectrum is somewhat similar to the 325 K one. A further reduction in temperature leads to a gradual decrease in intensity at ϵ_F —a pseudogap appears gradually as seen at 100 K—such pseudogap structure much below the SDW transition temperature (the SDW gap has already formed in the t_{2g} bands) is unusual. Ironically, while the pseudogap becomes more and more pronounced at lower temperatures, a sharp peak appears at ϵ_F below about 75 K (see Fig. 3(g)), which is independent of the error involved in the determination of ϵ_F —we have verified this by shifting ϵ_F within the error bar. Since the photoemission spectra probes the occupied part of the electronic structure and the feature at ϵ_F is the tail of the peak above ϵ_F , the peak width in the symmetrized data represent the lower bound, which would scale with the actual width. The enhancement of the peak intensity and the decrease in width with the decrease in temperature shown in the inset of Fig. 3(d) indicate Kondo like behavior.

Various recent studies⁹ showed signature of orbital Kondo effect in this compound—in such a case, the local moment formed due to the orbital degrees of freedom of Cr 3d electronic states are compensated by the conduction electrons forming a Kondo singlet as often observed in the case of spin moment. Such Kondo singlet formation will lead to a sharp peak near ϵ_F . The other explanation could be involving Shockley-type surface states, where the temperature dependence appears due to the strong electron-phonon coupling.^{9–11} However, it is already observed that the intensity of the surface states near ϵ_F reduces with the decrease in temperature. Thus, the sharp feature appearing at low temperatures is more likely to be associated to the Kondo compensation effect of Cr 3d orbital moment.

In summary, we have investigated the electronic structure of Cr using high resolution photoemission spectroscopy. The high resolution spectra exhibit signature of a pseudogap much below the spin density wave transition temperature and a sharp feature near the Fermi level is observed to grow at low temperature. These results manifest the microscopic details of the complex electronic properties observed in this system.

One of the authors S.P. thanks the Council of Scientific and Industrial Research, Government of India for financial support.

- ¹E. Fawcett, *Rev. Mod. Phys.* **60**, 209 (1988).
- ²A. Yeh, Y.-A. Soh, J. Brooke, G. Aeppli, T. F. Rosenbaum, and S. M. Hayden, *Nature* **419**, 459 (2002).
- ³F. Schiller, D. V. Vyalikh, V. D. P. Servedio, and S. L. Molodtsov, *Phys. Rev. B* **70**, 174444 (2004); E. Rotenberg, B. K. Freelon, H. Koh, A. Bostwick, K. Rossnagel, A. Schmid, and S. D. Kevan, *New J. Phys.* **7**, 114 (2005); E. Rotenberg, O. Krupin, and S. D. Kevan, *New J. Phys.* **10**, 023003 (2008).
- ⁴J. Schäfer, E. Rotenberg, S. D. Kevan, and P. Blaha, *Surf. Sci.* **454**, 885 (2000).
- ⁵G. Gewinner, J. C. Peruchetti, A. Jaéglé, and R. Pinchaux, *Phys. Rev. B* **27**, 3358 (1983).
- ⁶L. E. Klebanoff, S. W. Robey, G. Liu, and D. A. Shirley, *Phys. Rev. B* **30**, 1048(R) (1984).
- ⁷Z. Boekelheide, E. Helgren, and F. Hellman, *Phys. Rev. B* **76**, 224429 (2007); G. Adhikary, R. Bindu, S. Patil, and K. Maiti, *AIP Conf. Proc.* **1349**, 819 (2011).
- ⁸C. Pépin and M. R. Norman, *Phys. Rev. B* **69**, 060402(R) (2004).
- ⁹O. Yu. Kolesnychenko, R. de Kort, M. I. Katsnelson, A. I. Lichtenstein, and H. van Kempen, *Nature* **415**, 507 (2002); O. Yu. Kolesnychenko, G. M. M. Heijnen, A. K. Zhuravlev, R. de Kort, M. I. Katsnelson, A. I. Lichtenstein, and H. van Kempen, *Phys. Rev. B* **72**, 085456 (2005).
- ¹⁰T. Hänke, M. Bode, S. Krause, L. Berbil-Bautista, and R. Wiesendanger, *Phys. Rev. B* **72**, 085453 (2005).
- ¹¹M. Budke, T. Allmers, M. Donath, and M. Bode, *Phys. Rev. B* **77**, 233409 (2008).
- ¹²P. Blaha, K. Schwarz, G. K. H. Madsen, D. Kvasnicka, and J. Luitz, *WIEN2K, An Augmented Plane Wave + Local Orbitals Program for Calculating Crystal Properties* (Karlheinz Schwarz, Techn. Universität Wien, Austria, 2001).
- ¹³L. I. Johansson, L.-G. Petersson, K.-F. Berggren, and J. W. Allen, *Phys. Rev. B* **22**, 3294 (1980); J. Barth, F. Gerken, K. L. I. Kobayashi, J. H. Weaver, and B. Sonntag, *J. Phys. C* **13**, 1369 (1980).
- ¹⁴C. Guillot, Y. Ballu, J. Paigné, J. Lecante, K. P. Jain, P. Thiry, R. Pinchaux, Y. Pétrouff, and L. M. Falicov, *Phys. Rev. Lett.* **39**, 1632 (1977).
- ¹⁵S. Patil, S. K. Pandey, V. R. R. Medicherla, R. S. Singh, R. Bindu, E. V. Sampathkumaran, and K. Maiti, *J. Phys.: Condens. Matter* **22**, 255602 (2010); K. Maiti, S. Patil, and E. V. Sampathkumaran, *AIP Conf. Proc.* **1347**, 181 (2011).
- ¹⁶S. Raaen and V. Murgai, *Phys. Rev. B* **36**, 887 (1987).
- ¹⁷K. Maiti, U. Manju, S. Ray, P. Mahadevan, I. H. Inoue, C. Carbone, and D. D. Sarma, *Phys. Rev. B* **73**, 052508 (2006); K. Maiti, A. Kumar, D. D. Sarma, E. Weschke, and G. Kaindl, *Phys. Rev. B* **70**, 195112 (2004); K. Maiti and D. D. Sarma, *Phys. Rev. B* **61**, 2525 (2000); K. Maiti and R. S. Singh, *Phys. Rev. B* **71**, 161102(R) (2005); R. S. Singh, V. R. R. Medicherla, and K. Maiti, *Appl. Phys. Lett.* **91**, 132503 (2007).
- ¹⁸K. Maiti, R. S. Singh, and V. R. R. Medicherla, *Europhys. Lett.* **78**, 17002 (2007); K. Maiti, R. S. Singh, and V. R. R. Medicherla, *Phys. Rev. B* **76**, 165128 (2007).
- ¹⁹M. Kobayashi, K. Tanaka, A. Fujimori, S. Ray, and D. D. Sarma, *Phys. Rev. Lett.* **98**, 246401 (2007).